Accepted Manuscript

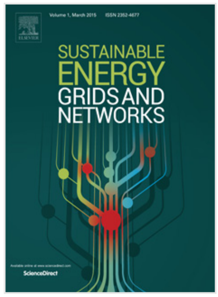

Wind turbine simulator fault diagnosis via fuzzy modelling and identification techniques

Silvio Simani, Saverio Farsoni, Paolo Castaldi

PII: S2352-4677(15)00006-5
DOI: http://dx.doi.org/10.1016/j.segan.2014.12.001
Reference: SEGAN 5

To appear in: *Sustainable Energy, Grids and Networks*

Received date: 21 September 2014
Revised date: 18 December 2014
Accepted date: 23 December 2014

Please cite this article as: S. Simani, S. Farsoni, P. Castaldi, Wind turbine simulator fault diagnosis via fuzzy modelling and identification techniques, *Sustainable Energy, Grids and Networks* (2015), http://dx.doi.org/10.1016/j.segan.2014.12.001

Available online at www.sciencedirect.com
ScienceDirect
SEGAN
ELSEVIER
Sustainable Energy, Grids and Networks 00 (2014) 1–13

Wind Turbine Simulator Fault Diagnosis via Fuzzy Modelling and Identification Techniques

Silvio Simani[a,*], Saverio Farsoni[a], Paolo Castaldi[b]

[a]*Department of Engineering, University of Ferrara, Ferrara, FE. 44122 Italy*
[b]*Electric and Informatics Department, University of Bologna, Bologna, Italy*

Abstract

For improving the safety and the reliability of wind turbine installations, the earliest and fastest fault detection and isolation is highly required, since it could be used also for accommodation purpose. Modern wind turbines consist of several important subsystems, which can be affected by malfunctions regarding actuators, sensors, and components. From the turbine control point–of–view they are extremely important since provide the actuation signals, the main functions, as well as the measurements. In this paper, a fault diagnosis scheme based on the identification of fuzzy models is described, in order to detect and isolated these faults in the most efficient way, in order also to improve the energy cost, the production rate, and reduce the operation and maintenance operations. Fuzzy systems are proposed here since the model under investigation is nonlinear, whilst the wind speed measurement is uncertain since it depends on the rotor plane wind turbulence effects. These fuzzy models are described as Takagi–Sugeno prototypes, whose parameters are estimated from the wind turbine measurements. The fault diagnosis methodology is thus developed using these fuzzy models, which are exploited as residual generators. The wind turbine simulator is finally employed for the validation of the obtained performances.

Keywords: Fuzzy modelling and identification, fault detection and isolation, residual generators, sustainability and availability, wind turbine benchmark.

1. Introduction

Modern industrial processes and controlled plants can exploit many technical resources comprising for example information sciences, real–time solutions, advanced diagnosis and control, and computational intelligence . This paper aims at reporting recent developments in the emerging areas of technology that find applications to factory advanced control and diagnosis, such as wind turbine installations.

The control tools normally used for improving the complete behaviour of power plants can exploit both advanced control schemes and complicated hardware solutions (for example, smart sensors, virtual actuators and processing units). This high complexity degree can increase the failure rate, thus motivating the requirement of an automatic scheme employed to quickly diagnose any abnormal working situations. These remarks raised a great interest in the issues of Fault Detection and Isolation (FDI) for dynamic systems, and many model–based strategies were suggested,

*Corresponding author.
Email address: silvio.simani@unife.it (Silvio Simani)
URL: www.silviosimani.it (Silvio Simani)

as described for example in [1, 2, 3, 4]. These methods rely on the mathematical description of the process under diagnosis. However, the diagnosis principle can be based on a limited number of approaches, *i.e.*: the parity space method, the state or output estimation, the Unknown Input Observer (UIO) principle, the Kalman Filters (KF) tool, the Unknown Input Kalman Filters (UIKF) strategy, and the parameter identification approach. Moreover, techniques relying on the artificial intelligence tools were also proposed [5]. Even if several linear and nonlinear methodologies were proposed, robust and reliable (in one word, "sustainable") FDI requires future researches.

It is worth noting that the accurate detection and isolation of faults can require a precise mathematical description of the plant under diagnosis, which can be expressed as state–space or input–output formulation. In this way, after the generation of the residual signals, their evaluation should guarantee the accurate fault detection, while avoiding the indication of false alarms generated by disturbance, measurement errors, and the model–reality mismatch. However, in actual conditions, the direct design and application of these FDI approaches can be difficult, motivated by the complexity of the mathematical description involved. This unavoidable complexity cannot allow the direct use of most of the linear FDI schemes, thus requiring a viable strategy for the direct application of the diagnosis schemes to practical examples [3, 6].

With reference to wind turbines, as considered in this work, many papers considered the model–based FDI problem [7, 8]. They showed that the more accurate the representation is at modelling the plant dynamics, the better its behaviour will be in diagnosing abnormal working situations.

This paper proposes the use of the fuzzy modelling and identification tool with application to a wind turbine benchmark for determining a straightforward solution of the FDI task. Two key issues of the proposed study are remarked. First, the model complexity does not imply the need of a complex mathematical description. In fact, as described here, the fuzzy modelling and identification tool can be exploited, thus avoiding purely nonlinear equations. Moreover, the mathematical description of the residual generators is derived via an identification approach. On the other hand, fuzzy prototypes as residual generators are designed, rather than purely nonlinear filters. This aspect is quite important when the designed diagnosis tool is proposed for real–time solutions. Moreover, the diagnosis scheme proposed in this study paper will be analysed in comparison with different approaches relying *e.g.* on banks of UIO/KF, as described in [1, 3].

This work proposes the use of the fuzzy logic theory, since it seems a simple tool able to manage complicated and unknown situations [9]. In particular, the residual generators applied to the wind turbine benchmark are derived as Takagi–Sugeno (TS) fuzzy descriptions [10], whose parameters are estimated via a system identification strategy. The efficacy of the suggested approaches are verified on the wind turbine benchmark measurements. Real–time simulations comprising realistic fault and working situations are used to assess the efficacy of the suggested methodologies.

It is worth noting that, with respect to the previous work by one of the same authors [11], this paper extends the results and improves the efficacy of the proposed solution. On the other hand, the identification approach, which is extended to the fuzzy framework and applied to the wind turbine data in this study, was developed by one of the same authors in [12]. Moreover, the design of the fuzzy estimators, which in this paper is exploited for the fault isolation task, was described in a paper by the same author [13], but applied to a diesel engine system.

Finally, the manuscript has the structure below. Section 2 addresses the wind turbine model exploited in the work. Section 3 describes the fuzzy modelling and identification tool used for FDI strategy development. The suggested FDI scheme is considered in Section 4. The obtained results reported in Section 5 serve to highlight the efficacy of the fuzzy tool, which is compared also with respect to a different FDI scheme. Section 6 concludes the work by summarising the main points of the paper and suggesting some future research issues.

2. Wind Turbine Simulated Model

The paper considers a realistic wind turbine with horizontal axis and three blades that move the rotor shaft due to the incoming wind flow. A gear–box is used for up–scaling the rotational speed of the power generator. More details of this benchmark wind turbine are available in [7]. Figure 1 provides the diagram of this power plant.

The converter torque $\tau_g(t)$ and the turbine blade pitch angle $\beta_r(t)$ are the two control inputs used to regulate the rotational speed $\omega_r(t)$ and the generated power $P_g(t)$. On the other hand, $\omega_g(t)$ represents the generator speed, whilst $\tau_g(t)$ is generator torque depending on the converter torque reference, $\tau_r(t)$. $\tau_{aero}(t)$ is the aerodynamic torque, whose estimate is computed from the wind speed, $v(t)$. However, this measurement is very uncertain, as shown *e.g.* in [7].

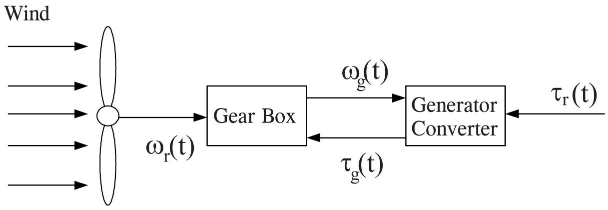

Figure 1. Wind turbine schematic diagram.

The aerodynamic description is provided by Eq. 1:

$$\tau_{aero}(t) = \frac{\rho\, A\, C_p\, (\beta_r(t),\ \lambda(t))\ v^3(t)}{2\, \omega_r(t)} \tag{1}$$

with the air density ρ, the turbine blade area A, the reference pitch angle $\beta_r(t)$, and the tip–speed ration $\lambda(t)$, described by Eq. 2:

$$\lambda(t) = \frac{\omega_r(t)\, R}{v(t)} \tag{2}$$

where the rotor radius is R. With reference to Eq. 1, the term C_p describes the power coefficient, that is usually represented by a two–dimensional map. Since the wind speed measurement $v(t)$ is uncertain, it is assumed that $\tau_{aero}(t)$ is affected by an error, which justifies the proposed approach of Section 3. The proposed scheme is able also to manage the nonlinearity described by the expressions of Eqs. 1 and 2.

The drive–train is described as a one–body model and the complete hydraulic pitch system is modelled as a second order transfer function [7]. Under these hypotheses, the overall continuous–time state–space model of the wind turbine process is described by Eq. 3:

$$\begin{cases} \dot{x}_c(t) &= f_c\,(x_c(t), u(t)) \\ \\ y(t) &= x_c(t) \end{cases} \tag{3}$$

where the available control inputs are represented by the vector $u(t) = \left[\beta_{1\,m_i}(t),\ \beta_{2\,m_i}(t),\ \beta_{3\,m_i}(t),\ \tau_g(t)\right]^T$ and the output measurements are described by the vector $y(t) = x_c(t) = \left[P_g(t),\ \omega_{g\,m_i}(t),\ \omega_{r\,m_i}(t)\right]^T$, respectively. These measurements are provided by two redundant sensor signals, with $i = 1, 2$. The static function $f_c\,(\cdot)$ describes the nonlinear relation between inputs and outputs. As described in Section 3, this nonlinear system will be approximated using the fuzzy models estimated from N data sequences $u(k)$ and $y(k)$, where $k = 1, 2, \ldots N$, are the sampling intervals.

With reference to the available redundant measurements from the benchmark, $\omega_{g\,m_i}$ and $\omega_{r\,m_i}$ represent the generator and rotor speed signals, respectively. $\beta_{j\,m_i}(t)$ refers to the i–th measurement of the j–th blade pitch. The look–up table $C_p\,(\beta, \lambda)$ is selected for describing a high–fidelity wind turbine, which is the test–rig for the validation of the proposed approach.

Finally, the measurement errors are described as Gaussian processes with statistics that represent realistic wind turbine measurement sensors.

2.1. Fault Mode and Effect Analysis

The benchmark system considered in this paper simulates a number of realistic faults, described in Table 1, which represent typical malfunctions of wind turbine installations. More details are available in [7].

In order to simplify the approach to the FDI task, the links between the fault situations reported above and the considered wind turbine measurements were considered and analysed. Therefore, Table 2 summarises the effects of the single faults on the inputs $\mathbf{u}(k)$ and outputs $y(k)$ signals acquired from the simulated process.

The results reported in Table 2 were achieved by using the so–called *Failure Mode & Effect Analysis* (FMEA) [14]. In particular, Table 2 shows the most sensitive input $u(k)$ or output $y(k)$ measurement with reference to the considered

Table 1. Fault scenario.

Fault	Description
1	Position sensor 1 of the pitch 1: stuck value
2	Position sensor 2 of the pitch 2: scaled value
3	Position sensor 1 of the pitch 3: stuck value
4	Rotor speed sensor 1: stuck value
5	Rotor speed sensor 2 & generator speed sensor 2: scaled values
6	Pitch 2 actuator: changed dynamics due to air content in the hydraulic circuit
7	Pitch 3 actuator: changed dynamics due to hydraulic circuit low pressure
8	Converter torque control: offset value
9	Drive train: changed dynamics

Table 2. Results of the FMEA approach.

Measurements	Fault
$\beta_{1\,m_1}(t)$	1
$\beta_{2\,m_2}(t)$	2
$\beta_{3\,m_2}(t)$	3
$\beta_{1\,m_2}(t)$	4
$\beta_{2\,m_1}(t)$	5
$\omega_{r\,m_1}(t)$	6
$\omega_{r\,m_2}(t)$	7
$P_g(t)$	8
$\omega_{r\,m_1}(t)$	9

fault situations. Obviously, fault conditions different from the ones considered in this paper could probably require different measurements. The approach is similar to the procedure shown in [13, 12], and it represents an important key point, since it simplifies the fault isolation task, described in Section 4, and the set of measurement inputs and outputs to be used for identification purpose, recalled in Section 3.

3. Fuzzy Modelling and Identification

This section addresses the derivation of the residual generators used for the wind turbine benchmark FDI. In particular, the parameter estimation method summarised in the following enhances the development of the suggested FDI scheme reported in Section 4.

The TS fuzzy prototype consists of a set of rules R_i, where the consequents are deterministic functions f_i:

$$R_i : \text{ IF } x \text{ is } A_i \text{ THEN } y_i = f_i\big(x\big) \tag{4}$$

where $i = 1, 2, \ldots, K$, with K the number of rules (or clusters). The term x describes the antecedent variables, whilst y_i represents the consequent outputs. The fuzzy set A_i of the i–th rule is represented with a (multivariable) membership function, as described *e.g.* in [9].

The terms f_i are properly parametric models, whose structure is fixed, and only its parameters can vary. These functions exploited in this study have the affine form of Eq. 5:

$$y_i = a_i\, x + b_i, \tag{5}$$

with a_i and b_i represent the model parameters. These models are proposed in this study as they are able to approximate nonlinear systems with an arbitrary degree of accuracy [15].

When the degree of fulfilment of the antecedent $\lambda_i(x) = \mu_{A_i}(x)$ is computed, the complete TS model is represented with the expression:

$$y = \frac{\sum_{i=1}^{K} \lambda_i(x)\, y_i}{\sum_{i=1}^{K} \lambda_i(x)} \tag{6}$$

where the membership functions λ_i are usually described with exponential functions [9]. Section 5 will show that exponential membership functions represent the optimal choice for the accurate description of the fuzzy cluster shapes.

It is worth noting that the TS model of Eq. 4 can approximate a dynamic system if the consequents are described as linear autoregressive models $x(k) = [y(k-1), \cdots, y(k-n), u(k-1), \cdots, u(k-n)]^T$, and $a_i = [\alpha_1^{(i)}, \cdots, \alpha_n^{(i)}, \delta_1^{(i)}, \cdots, \delta_n^{(i)}]$, with n is the memory (order) of the system. When the structure of Eq. 6 is considered, a methodology developed in [16] is exploited for the identification of both a_i, b_i, and the model order n.

On the other hand, the membership degrees λ_i of Eq. 6 are easily estimated using the fuzzy clustering procedure described in [9]. In particular, this work proposes to use the fuzzy c–means clustering method developed in [9] and already available as ready–to–use program. Moreover, this clustering tool choice is it can be directly integrated with the estimation scheme suggested by one of the authors in [16]. The issue of the estimation of the optimal number of clusters K was considered *e.g.* in in [16, 17].

The remainder of this section summarises the procedure for the estimation of the TS fuzzy model parameters from noisy data.

Several techniques for the estimation of the model parameters a_i and b_i in Eq. 5 are available. However, if it is assumed that errors affect both the regressor and the regressand variables, the optimal parameters are identified by exploiting a scheme known as Errors–In–Variables (EIV) approach [18]. In fact, it can be considered here since it leads to the minimisation of the estimation (or prediction) errors of the K independent local affine models [17].

To this aim, with reference to the i–th cluster ($i = 1, \cdots, K$), the data matrices are built as follows:

$$X_n^{(i)} = \begin{bmatrix} y(k) & x_n^T(0) & 1 \\ y(k+1) & x_n^T(1) & 1 \\ \vdots & \vdots & \\ y(k+N_i-1) & x_n^T(N_i-1) & 1 \end{bmatrix} \tag{7}$$

with n representing the number of delayed inputs and outputs, *i.e.* $x_n(h) = [y(h-1), \cdots, y(h-n), u(h-1), \cdots, u(h-n)]^T$. Moreover:

$$\Sigma_n^{(i)} = \left(X_n^{(i)}\right)^T X_n^{(i)}. \tag{8}$$

The problem of noise rejection is thus solved with the assumption that the measurement noise represented by the signals $\tilde{u}(k)$ and $\tilde{y}(k)$ are additive on the input and output measurements $u^*(k)$ and $y^*(k)$, with a number of sampling instant $k = 1, 2, \cdots, N$. In this situation, the positive–definite covariance matrix $\Sigma_n^{(i)}$ related to the data of the i–th cluster can be described as the contribution of two addenda, that is $\Sigma_n^{(i)} = \Sigma_n^{*(i)} + \bar{\tilde{\Sigma}}_n$.

In particular, the covariance matrix $\bar{\tilde{\Sigma}}_n$ has the form:

$$\bar{\tilde{\Sigma}}_n = \text{diag}[\bar{\tilde{\sigma}}_y I_{n+1}, \bar{\tilde{\sigma}}_u I_n, 0] \geq 0. \tag{9}$$

This identification problem is solved by computing the unknown noise variance values $\bar{\tilde{\sigma}}_u$ and $\bar{\tilde{\sigma}}_y$ that derive from Eq. 10:

$$\Sigma_n^{*(i)} = \Sigma_n^{(i)} - \tilde{\Sigma}_n \geq 0. \tag{10}$$

which is a function of the unknowns $\tilde{\sigma}_u$ and $\tilde{\sigma}_y$ and $\tilde{\Sigma}_n = \text{diag}[\tilde{\sigma}_y I_{n+1}, \tilde{\sigma}_u I_n, 0]$. Actually, the parameters of the local affine model are estimated by determining the noise variances $(\tilde{\sigma}_u, \tilde{\sigma}_y) \in \Gamma_{n+1}^{(i)} = 0$ making the matrix $\Sigma_{n+1}^{*(i)}$ close to the double singular condition. However, in each i–th cluster, different noise variances $(\bar{\tilde{\sigma}}_u^{(i)}, \bar{\tilde{\sigma}}_y^{(i)})$ are assumed, and the following expression is derived:

$$\Sigma_n^{*(i)} = \Sigma_n^{(i)} - \tilde{\Sigma}_n^{(i)} \geq 0 \tag{11}$$

with $\tilde{\Sigma}_n^{(i)} = \text{diag}[\bar{\tilde{\sigma}}_u^{(i)} I_{n+1}, \bar{\tilde{\sigma}}_y^{(i)} I_n, 0]$. The values $(\bar{\tilde{\sigma}}_u^{(i)}, \bar{\tilde{\sigma}}_y^{(i)})$ represent the additive noise variance values of the data in the i–th cluster.

These assumptions mean that the following relations normally hold [19, 16]:

$$\begin{cases} u(k) &= u^*(k) + \tilde{u}(k) \\ y(k) &= y^*(k) + \tilde{y}(k) \end{cases} \tag{12}$$

where $u^*(k)$ and $y^*(k)$ represent the data without noise, whilst the noise signals $\tilde{u}(k)$ and $\tilde{y}(k)$ do not depend on other terms. Moreover, only the measurements $u(k)$ and $y(k)$ are available.

Finally, the matrices $\tilde{\Sigma}_n^{(i)}$ are derived and the model parameters for the i–th cluster are estimated via the expression:

$$\left(\Sigma_n^{(i)} - \tilde{\Sigma}_n^{(i)}\right) a^{(i)} = 0 \tag{13}$$

with $i = 1, \ldots, K$, and a number of K clusters. This identification approach will be exploited for the estimation of the residual generators for FDI as described in Section 4.

4. Fault Diagnosis Strategy

The issue of the residual generator design for the FDI of the wind turbine model will be addressed in this section. It wind turbine system is assumed to be modelled by the description of Eq. 3. $u(k)$ and $y(k)$ represent the controlled inputs and the system outputs, respectively. The so–called model–reality mismatch in fault–free conditions can be represented by the difference $y(k) - \hat{y}(k)$. It could take into account measurement errors, parameter variations, and disturbance. The reconstruction of the measurement $y(k)$, *i.e.* $\hat{y}(k)$ is obtained from an identified model of Eq. 6. According to the description of Eq. 12, in practice, the signals $u^*(k)$ and $y^*(k)$ are acquired by measurement sensors, which are inevitably affected by errors.

On the other hand, if the sensor dynamics are neglected, also faults affect the measurement process, which is thus modelled as:

$$\begin{cases} u(k) &= u^*(k) + f_u(k) \\ y(k) &= y^*(k) + f_y(k) \end{cases} \tag{14}$$

where the terms $f_u(k)$ and $f_y(k)$ are additive fault signals.

Regarding the FDI task, this paper proposed to use TS fuzzy prototypes that are exploited for residual generators from the redundant input and output signals $u(k)$ and $y(k)$. In this way, Fig. 2 shows that proper residual signals are computed as:

$$r(k) = \hat{y}(k) - y(k). \tag{15}$$

i.e. the different between the actual $y(k)$ and its reconstruction $\hat{y}(k)$.

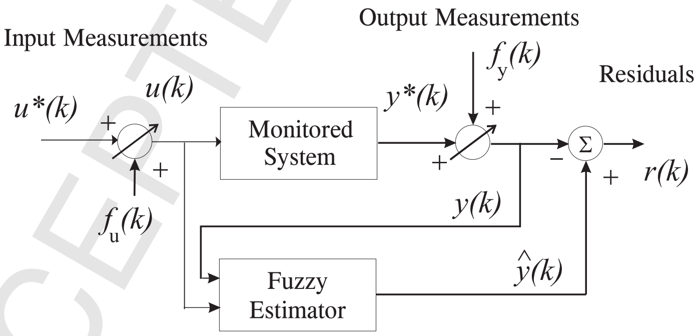

Figure 2. The generation of the residual signals for FDI.

After the residual generation task, its evaluation is performed for detecting any fault occurrence, and for isolating the faulty actuator or sensor signals.

A direct geometric threshold comparison is proposed here to perform the fault detection stage. However, a detection delay can be present due to the fault modes summarised in Section 2.1. The fault detection logic is performed according to the test described by Eqs. 16:

$$\begin{cases} \bar{r} - \delta\,\sigma_r \leq r(k) \leq \bar{r} + \delta\,\sigma_r \\ \text{if fault–free} \\ \\ r(k) < \bar{r} - \delta\,\sigma_r \ \text{ or } \ r(k) > \bar{r} + \delta\,\sigma_r \\ \text{if faulty} \end{cases} \tag{16}$$

Actually, the residual $r(k)$ is modelled as a stochastic variable, whose mean and variance values are estimated with the relations of Eqs. 17:

$$\begin{cases} \bar{r} = \frac{1}{N}\sum_{k=1}^{N} r(k) \\ \\ \sigma_r^2 = \frac{1}{N}\sum_{k=1}^{N} \left[r(k) - \bar{r}\right]^2 \end{cases} \tag{17}$$

where the terms $\bar{r}$ and σ_r^2 represents the mean and variance values of the fault–free residual samples, respectively. In Eqs. 17 the sample number of $r(k)$ is N. Note that $\bar{r}$ and σ_r^2 could be exactly computed from the $r(k)$ statistics, usually unknown.

A robustness and reliability degree is introduced for distinguishing the normal and the faulty behaviours, which is represented by the tolerance parameter δ (normally $\delta \geq 2$). A technique developed in [20] by one of the same authors is applied here not to obtain conservative results. In particular, extensive simulations lead to the optimal value of δ that minimises the false alarm probability and maximise the true detection rate. This topic will be further analysed in Section 5.

The second issue concerns the fault isolation task, and it is achieved using a bank of residual generators properly designed, which resembles the Generalised Observer Scheme (GOS) [1]. This task can be easily solved here as Section 2.1 showed how different faults $f_y(k)$ or $f_u(k)$ affect different input or output measurements. In this way, when the outputs are fault–free, $f_u(k)$ possibly affecting one of the inputs $u(k)$, is diagnosed with a bank of TS fuzzy estimators of Eq. 6, as depicted in Fig. 3.

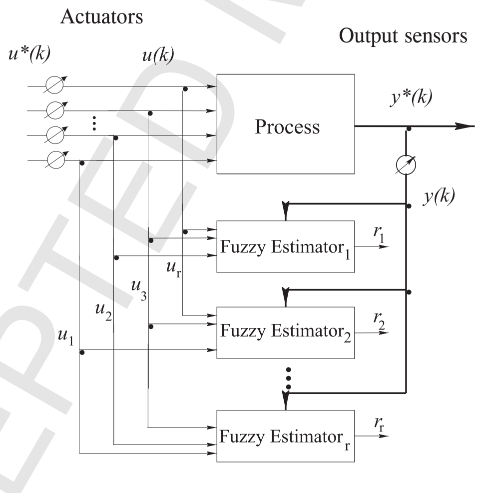

Figure 3. Scheme for the isolation of input faults.

The number of residual generators coincides with the number of faults to be diagnosed. Fig. 3 shows that the i–th residual generator is fed by all but the i–th input measurement (or even more input signals, if necessary) and all output measurements. The generated residual signal is thus sensitive to all but the i–th fault $f_u(k)$. These residual generators are described by fuzzy TS models that are identified with the strategy reported in Section 3. In particular, the i–th fuzzy estimator that does not depend on the i–th input measurement is identified using $y(k)$ and all but the i–th input measurement $u_i(k)$ $(i = 1, \ldots, r)$.

On the other hand, when the input variables are fault–free, a fault $f_y(t)$ affecting the output measurement is diagnosed with an output fuzzy estimator bank, which are organised as in Fig. 3.

The efficacy of the overall fault isolation scheme is summarised in Table 3, where the so–called "fault signatures" are summarised for the single fault case regarding each input–output signal. It is worth noting that the residuals r_i of Fig. 3 are indicated by r_{I_i} or r_{O_i} in Table 3 if they are generated by the bank for input or output sensor fault isolation, respectively.

Table 3. Fault signatures.

	u_1	u_2	$\ldots$	u_r	y_1	y_2	$\ldots$	y_m
r_{I_1}	0	1	$\ldots$	1	1	1	$\ldots$	1
r_{I_2}	1	0	$\ldots$	1	1	1	$\ldots$	1
$\vdots$	$\vdots$	$\vdots$	$\vdots$	$\vdots$	$\vdots$	$\vdots$	$\vdots$	$\vdots$
r_{I_r}	1	1	$\ldots$	0	1	1	$\ldots$	1
r_{O_1}	1	1	$\ldots$	1	1	0	$\ldots$	0
r_{O_2}	1	1	$\ldots$	1	0	1	$\ldots$	0
$\vdots$	$\vdots$	$\vdots$	$\vdots$	$\vdots$	$\vdots$	$\vdots$	$\vdots$	$\vdots$
r_{O_m}	1	1	$\ldots$	1	0	0	$\ldots$	1

With reference to Table 3, an entry '1' means that the residual is affected by the fault, whilst '0' indicates that the corresponding residual does not depend on the particular fault.

Finally, according to Table 3, it is worth noting that multiple faults are isolable, as only the i–th output signal feeding the residual generator of r_{O_i} is affected by the fault on y_i. On the other hand, multiple faults on the inputs u_i are not isolable as the residuals r_{I_i} depend on the faults affecting different inputs.

5. Simulated Results

The suggested identification and FDI approach was applied to the benchmark summarised in Section 2. The data exploited for identification purpose were $N = 440 \times 10^3$ samples acquired with a sampling rate of 100 Hz.

5.1. Wind Turbine Modelling and FDI

As addressed in Section 3, the data clustering algorithm with $K = 4$ fuzzy sets and $n = 2$ was employed. After this fuzzy c–means clustering, the residual generator parameters $\mathbf{a}_i$ and b_i $(i = 1, \cdots, K)$ were identified according to Section 3. In particular, Fig. 3, highlighted that the residual signals for FDI were computed using a bank of 5 TS fuzzy estimators of Eq. 6. Table 2 suggested that this approach is able to diagnose the faults 1, 2, 3, 4, and 5, according to Fig. 3. Moreover, by following again the results of Table 2, a bank of 4 fuzzy residual generators allowed the diagnosis of the faults 6, 7, 8, and 9. Note that the membership functions β_i used in Eq. 6 were estimated as Gaussian functions, and derived from the same fuzzy c–means clustering approach [21].

In the following, the simulation results regarding the fault 4, *i.e.* $f_u(t)$, commencing at the instant $t = 1500$ s. are shown. Moreover, the fault 8 corresponding to $f_y(t)$ is also presented. This fault is active between the time instants 3800 s. and 3900 s. These faults change the measurements $u(t)$ and $y(t)$, and therefore affect the residuals $r_{I_i}(t)$ generated by the residual generator of Eq. 6. These residual signals are compared with fixed thresholds according to Eq. 16. As an example, Fig. 4 shows the fault–free $y(k)$ (grey dashed line) and the faulty $\hat{y}(k)$ (black continuous line) signals regarding the $\omega_r(t)$ measurement from the device of Fig. 2. On the other hand, Fig. 5 compares the corresponding fault–free residual $r_{I_i}(t)$ (grey dashed line) with the corresponding faulty one (black continuous line) generated by the device of Fig. 3.

Fig. 5 also depicts the FDI thresholds of Eqs. 16 using dotted constant lines. In the following, a simulation tool will be described for determining their values in order to minimise both the false alarm rate and the missed fault

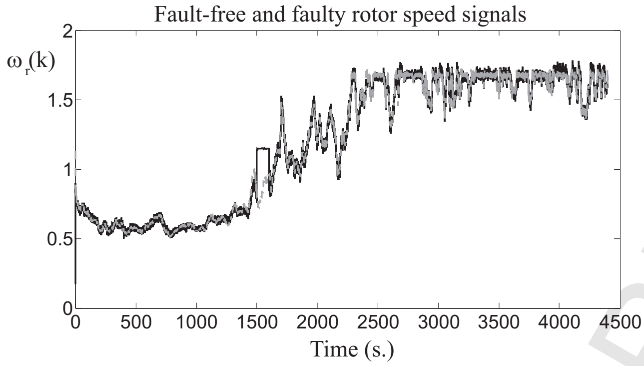

Figure 4. The signals $\hat{y}(k)$ and $\hat{y}(k)$for the fault 4.

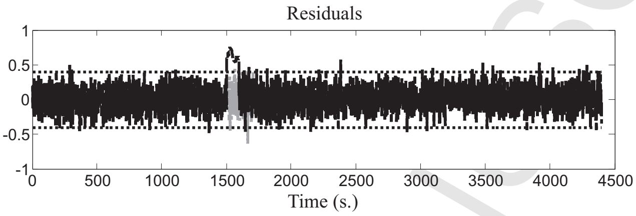

Figure 5. The residuals $r_{I_i}(t)$ for the fault 4.

probability, as well as to maximise the correct FDI rates. Therefore, the diagnosis of the considered faults is correctly performed if the corresponding residuals exceed these thresholds, as shown in Fig. 5.

With reference to the fault 8, *i.e.* $f_y(t)$ considered here, Fig. 6 shows the fault–free $y(k)$ (grey dashed line) and the faulty $\hat{y}(k)$ (black continuous line) signals concerning the $\tau_g(t)$ measurement from the device of Fig. 2.

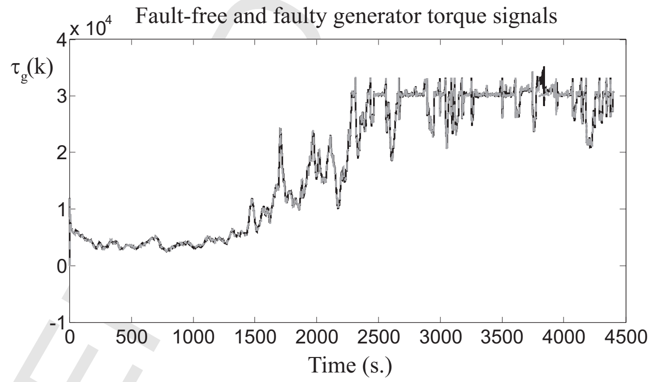

Figure 6. The signals $y(k)$ and $\hat{y}(k)$ for the fault 8.

On the other hand, Fig. 7 depicts the fault–free residual with grey dashed line and the faulty residual in black continuous line.

Also in this case, Fig. 7 reports also the FDI thresholds as dotted constant lines. They were optimally selected in order to achieve the minimisation of the false alarm rate and the missed fault probability. Note that the obtained results show the efficacy of the proposed FDI methodology relying on fuzzy residual generator functions identified

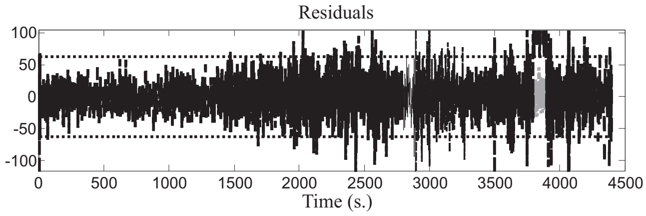

Figure 7. The residual signals $r_{O_i}(t)$ for the fault 8.

from uncertain measurements generated by the wind turbine benchmark.

5.2. FDI Comparisons

This section reports the comparison of the proposed strategy with respect to a different FDI approach. In particular, the features of the FDI method developed in this study are analysed by considering an Unknown Input Kalman Filters (UIKF) bank proposed *e.g.* in [1]. These UIKF devices used as residual generators were obtained from a linear state–space description of the wind turbine benchmark, and designed as described *e.g.* in [22, 23]. However, the fuzzy multiple–model identification was not exploited here. The achieved results are summarised in Table 4, which reports if the considered faults are isolable and their FDI delays.

Table 4. FDI features of the UIKF bank.

Fault	Fault Isolation	FDI delay
1	Yes	15.98s.
2	Yes	95.89s.
3	Yes	20.61s.
4	Yes	10.34s.
5	Yes	91.14s.
6	No	55.71s.
7	No	55.65s.
8	No	18.98s.
9	No	12.68s.

With reference to the results of Table 4, note that model–based schemes should be used if accurate descriptions of the process models are available. Moreover, the UIKF solution can manage the disturbance rejection problem by exploiting complex design algorithms. However, Table 4 shows that the UIKF fault sensitivity is lower than the fuzzy predictors. On the other hand, the advantage of the proposed fuzzy approach relies in its simplicity, even if a suitable FDI threshold selection procedure can be required, as sketched in the remainder of this section.

5.3. FDI Performance Evaluation

To this aim, further simulation are shown for achieving the optimal performance and evaluating the features of the proposed FDI scheme with reference to the model–reality mismatch and the measurement errors. Thus, extensive experiments were realised by using the wind turbine simulator of Section 2 the Monte–Carlo tool. In fact, this methodology is extremely powerful here since the FDI effectiveness is a function of the residual signals sensitivity with respect to the model uncertainty and the measurement accuracy.

Section 4 highlighted that the input and output sequences $u(k)$ and $y(k)$ can be generated with arbitrary measurement errors and noise levels. Therefore, the evaluation of the achievable performance is based on properly computed indices, which were motivated by previous studies, see *e.g.* [24, 25]. They were evaluated using 1000 Monte–Carlo simulations, and empirically computed as:

- False Alarm Rate (FAR): the ratio between the number of wrongly detected faults and the number of simulated faults;
- Missed Fault Rate (MFR): the ratio between the total number of missed faults and the total number of considered faults;
- True FDI Rate, (TFDIR): the ratio between the number correctly diagnosed faults and the total number of occurred faults;
- Mean FDI Delay, (MFDID): the average FDI delay interval.

Table 5 reports the evaluation of these indices when the fuzzy predictors proposed here are considered and the optimal δ in Eq. 16 was selected.

Table 5. Monte–Carlo analysis with the fuzzy estimators.

Fault	FAR	MFR	TFDIR	MFDID	δ
1	0.002	0.003	0.997	0.03s.	3.8
2	0.001	0.001	0.999	0.47s.	4.3
3	0.002	0.003	0.997	0.06s.	4.2
4	0.002	0.003	0.997	0.04s.	4.5
5	0.001	0.001	0.999	0.03s.	3.7
6	0.002	0.003	0.997	0.73s.	4.4
7	0.002	0.003	0.997	0.61s.	4.3
8	0.001	0.001	0.999	0.03s.	3.5
9	0.002	0.003	0.998	0.15s.	3.9

Table 5 highlights that the optimal values of δ in Eq. 16 allows to obtain FAR and MFR values lower than 0.3%, with TFDIR larger than 99.7%, with minimal MFDID times. This aspect represents one of the key issues of the suggested strategy, which demonstrates the efficacy of the Monte–Carlo tool exploited here for the evaluation of the robustness issue of the suggested methodology. The simulation tests seem also able also to enhance the designer to assess the reliability feature of designed FDI strategy when applied to more realistic examples.

5.4. Hardware–In–the–Loop Experiments

For the evaluation of more realistic working conditions, since real data from a wind turbine are not available, this section summarises the results achieved using an Hardware In the Loop (HIL) setup. The procedure serves also to highlight the performance of the designed software algorithms realising the proposed FDI strategy and working in an real–time conditions when implemented on–board the wind turbine installation. Figure 8 describes the schematic diagram of the HIL test–rig.

This test–rig was already presented in [11] but for control performance evaluation. The setup consists of an industrial computer that provides the modelling of the wind turbine dynamics in the Labview® environment. The FDI strategy suggested in this study was implemented using the AWC 500 system with its on–board electronics and interface circuits, which simulate the data acquisition and transmission processes. Table 6 summarises the results obtained using this real–time laboratory setup.

Table 6 highlights the consistency of the almost real–time tests with respect to the results shown in Table 5 from the Monte–Carlo simulation tool. In fact, note that the performances of Table 5 seem better than the HIL tests in Table 6. However, the numerical implementation precision of the on–board processor and the signal processing electronics motivate possible deviations between the achieved results, which seem quite accurate when almost real–time wind turbine experimental applications are experimented with.

Finally, note that the main challenge in this application area is to reduce the energy cost allowed by the presented fault diagnosis strategy, without significantly increasing the cost of the installation operations. In this way, the cost of the energy can be decreased by about 2%, mainly due to an increase in the system reliability. Furthermore, the wind turbine availability will be increased correspondingly, by the features of the diagnosis scheme developed in the

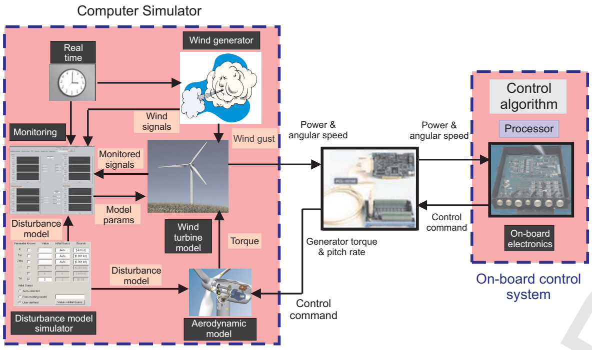

Figure 8. Main elements of the HIL test–bed.

Table 6. HIL laboratory setup FDI results.

Fault	FAR	MFR	TFDIR	MFDID	δ
1	0.005	0.005	0.995	0.07s.	4.1
2	0.004	0.004	0.996	0.49s.	4.5
3	0.004	0.004	0.996	0.08s.	4.6
4	0.005	0.005	0.995	0.07s.	4.8
5	0.003	0.004	0.997	0.06s.	3.9
6	0.004	0.005	0.996	0.76s.	4.8
7	0.005	0.004	0.995	0.64s.	4.5
8	0.005	0.004	0.995	0.06s.	3.8
8	0.004	0.005	0.996	0.18s.	4.3

paper, which allows to achieve the objective of decreasing lost production factor by 10%. This thus leads to an impact on increasing the attractiveness of the wind turbine technology by improve the cost and increasing reliability and availability.

6. Conclusion

This paper suggested a viable approach for the development of a fault diagnosis scheme with application to a wind turbine benchmark. The scheme relies on fuzzy prototypes that are identified from uncertain input–output data measurements. The process under diagnosis is nonlinear and the acquired measurements are affected by errors due to the wind speed uncertain knowledge. These identified fuzzy models were used for robust residual generation. The estimation procedure used for deriving the fuzzy model parameters exploited a data fuzzy clustering tool and a system identification algorithm solving the noise–rejection problem. The efficacy of this approach was investigated also in real–time conditions and comparisons with a different fault diagnosis highlighted the key features of the proposed methodology. In this way, by considering wind turbine standard installations, with typical costs and production rates, the fault diagnosis scheme presented here could be able to reduce the lost production factor with at least 10%, and to decrease the cost of energy by 2%, due to the decrease of unexpected and unplanned the maintenance operations, representing the most expensive costs for wind turbines.

References

[1] J. Chen, R. J. Patton, Robust Model–Based Fault Diagnosis for Dynamic Systems, Kluwer Academic Publishers, Boston, MA, USA, 1999.
[2] R. Isermann, Fault–Diagnosis Systems: An Introduction from Fault Detection to Fault Tolerance, 1st Edition, Springer–Verlag, Weinheim, Germany, 2005, ISBN: 3540241124.

[3] S. Simani, C. Fantuzzi, R. J. Patton, Model-based fault diagnosis in dynamic systems using identification techniques, 1st Edition, Vol. 1 of Advances in Industrial Control, Springer–Verlag, London, UK, 2003, ISBN: 1852336854.
[4] S. X. Ding, Model–based Fault Diagnosis Techniques: Design Schemes, Algorithms, and Tools, 1st Edition, Springer, Berlin Heidelberg, 2008, ISBN: 978–3540763031.
[5] J. Korbicz, J. M. Koscielny, Z. Kowalczuk, W. Cholewa (Eds.), Fault Diagnosis: Models, Artificial Intelligence, Applications, 1st Edition, Springer–Verlag, London, UK, 2004, ISBN: 3540407677.
[6] B. Benini, P. Castaldi, S. Simani, Fault Diagnosis for Aircraft System Models: An Introduction from Fault Detection to Fault Tolerance, 1st Edition, VDM Verlag Dr. Müller Aktiengesellschaft & Co. KG., Dudweiler Landstr, 99. 66123 – Saarbrücken, Germany, 2009, ISBN: 978–3–639–21364–5. http://www.vdm-publishing.com/.
[7] P. F. Odgaard, J. Stoustrup, M. Kinnaert, Fault–Tolerant Control of Wind Turbines: A Benchmark Model, IEEE Transactions on Control Systems Technology 21 (4) (2013) 1168–1182, ISSN: 1063–6536. DOI: 10.1109/TCST.2013.2259235.
[8] P. F. Odgaard, J. Stoustrup, Unknown Input Observer Based Scheme for Detecting Faults in a Wind Turbine Converter, in: Proceedings of the 7th IFAC Symposium on Fault Detection, Supervision and Safety of Technical Processes, Vol. 1, IFAC – Elsevier, Barcelona, Spain, 2009, pp. 161–166, DOI: 10.3182/20090630–4–ES–2003.0048.
[9] R. Babuška, Fuzzy Modeling for Control, Kluwer Academic Publishers, Boston, USA, 1998.
[10] T. Takagi, M. Sugeno, Fuzzy identification of systems and its application to modeling and control, IEEE Transaction on System, Man and Cybernetics SMC-15 (1) (1985) 116–132.
[11] S. Simani, Application of a Data–Driven Fuzzy Control Design to a Wind Turbine Benchmark Model, Advances in Fuzzy Systems 2012 (Web: http://www.hindawi.com/journals/afs/2012/504368/) (2012) 1–12, invited paper for the special issue: Fuzzy Logic Applications in Control Theory and Systems Biology (FLACE) . ISSN: 1687–7101, e–ISSN: 1687-711X. DOI: 10.1155/2012/504368.
[12] S. Simani, R. J. Patton, Fault diagnosis of an industrial gas turbine prototype using a system identification approach, Control Engineering Practice 16 (7) (2008) 769–786, Publisher: Elsevier Science. ISSN: 0967–0661. DOI: 10.1016/j.conengprac.2007.08.009.
[13] S. Simani, Residual Generator Fuzzy Identification for Automotive Diesel Engine Fault Diagnosis, International Journal of Applied Mathematics and Computer Science – AMCS 23 (2) (2013) 419–438, Invited Contribution to the AMCS Quarterly. Organisers: Koscielny, M. J. and Syfert, M. ISSN: 1641–876X. DOI: 10.2478/amcs–2013–0032.
[14] D. H. Stamatis, Failure Mode and Effect Analysis: FMEA from Theory to Execution, 2nd Edition, ASQ Quality Press, Milwaukee, WI, USA, 2003, ISBN: 0873895983.
[15] C. Fantuzzi, R. Rovatti, On the approximation capabilities of the homogeneous Takagi–Sugeno model, in: Proceedings of the Fifth IEEE International Conference on Fuzzy Systems, New Orleans, LA, USA, 1996, pp. 1067–1072.
[16] S. Simani, C. Fantuzzi, R. Rovatti, S. Beghelli, Parameter identification for piecewise linear fuzzy models in noisy environment, International Journal of Approximate Reasoning 1 (22) (1999) 149–167, Publisher: Elsevier.
[17] C. Fantuzzi, S. Simani, S. Beghelli, R. Rovatti, Identification of piecewise affine models in noisy environment, International Journal of Control 75 (18) (2002) 1472–1485, Publisher: Taylor and Francis, Ltd.
[18] S. Van Huffel, P. Lemmerling (Eds.), Total Least Squares and Errors–in–Variables Modeling: Analysis, Algorithms and Applications, 1st Edition, Springer–Verlag, London, UK, 2002, ISBN: 1402004761.
[19] R. Rovatti, C. Fantuzzi, S. Simani, High–speed DSP–based implementation of piecewise–affine and piecewise–quadratic fuzzy systems, Signal Processing Journal. Publisher: Elsevier 80 (6) (2000) 951–963, (Special Issue on Fuzzy Logic applied to Signal Processing).
[20] S. Simani, M. Bonfè, P. Castaldi, W. Geri, Residual Generator Design and Performance Evaluation for Aircraft Simulated Model FDI, in: IEEE (Ed.), CCA 2007. 16th IEEE International Conference on Control Applications, Vol. CD–Rom, IEEE, 2007 Omnipress IEEE, Singapore, Malaysia, 2007, pp. 1043–1048, Part of IEEE Multi–Conference on Systems and Control. DOI: 10.1109/CCA.2007.4389371. ISBN: 1–4244–0443–6. ISSN: 1085–1992.
[21] R. Babuška, Fuzzy Modelling and Identification Toolbox, Control Engineering Laboratory, Faculty of Information Technology and Systems, Delft University of Technology, Delft, The Netherlands, version 3.1 Edition, (Available at http://lcewww.et.tudelft.nl/ ˜babuska) (2000).
[22] S. Simani, C. Fantuzzi, S. Beghelli, Diagnosis techniques for sensor faults of industrial processes, IEEE Transactions on Control Systems Technology 8 (5) (2000) 848–855.
[23] S. Simani, Fault Diagnosis of a Simulated Industrial Gas Turbine via Identification Approach, International Journal of Adaptive Control and Signal Processing 21 (4) (2007) 326–353, copyright 2006 John Wiley & Sons, Ltd. ISSN: 0890–6327. DOI: 10.1002/acs.924.
[24] R. J. Patton, F. J. Uppal, S. Simani, B. Polle, Reliable fault diagnosis scheme for a spacecraft attitude control system, Journal of Risk and Reliability 222 (2) (2008) 139–152, 6th IFAC SAFEPROCESS Special Issue. Publisher: Professional Engineering Publishing. Proceedings of the Institution of Mechanical Engineers, Part O. ISSN: 1748-006X (Print) 1748-0078 (Online). DOI: 10.1243/1748006XJRR98.
[25] R. J. Patton, F. J. Uppal, S. Simani, B. Polle, Robust FDI applied to thuster faults of a satellite system, Control Engineering Practice 18 (9) (2010) 1093–1109, ACA'07 – 17th IFAC Symposium on Automatic Control in Aerospace Special Issue. Publisher: Elsevier Science. ISSN: 0967–0661. DOI: 10.1016/j.conengprac.2009.04.011.